

# Characterization and Mechanical Properties of Flame Sprayed Hydroxyapatite/Polymer Composite Coatings

L. Sun, C. C. Berndt  
Center for Thermal Spray Research, State University of New York  
at Stony Brook, Stony Brook, NY, 11794-2275 USA

K. A. Gross  
Department of Materials Engineering, Monash University, Victoria 3800 Australia

## Abstract

**Hydroxyapatite/polymer** composite coatings of different volume ratios were produced using a Plastic Flame Spray (PFS) system. The intent of this processing is to obtain a coating with an optimal combination of biological and mechanical properties of these two materials for skeletal implants. The composite coatings were produced with a mechanical blend of EMMA and hydroxyapatite powder from a fluidized bed powder feeder. Characterization was conducted by scanning electron microscopy on the surface morphology, polished cross-sections and fracture surface morphology of the coatings. The bioactivity of the coatings was evaluated with a calcium ion meter, and the stress-strain behavior was investigated by tensile testing. The biological and mechanical properties were found to be related to the volume and the distribution of the hydroxyapatite in the polymer matrix.

## Introduction

Hydroxyapatite (HA) coating on metal implants have been developed for superior bioactivity and osteoconductivity of the HA, resulting in faster and stronger bone-implant fixation **within** the clinical setting over the last decade. However, like other current skeletal prostheses, this system is also susceptible to stress shielding of the bone at the bone-implant interface due to the great difference of modulus between the implant (106 **GPa** for Ti-6Al-4V, 8-120 **GPa** for hydroxyapatite) and the bone (7-30 **GPa** for cortical bone). [1,2] This stress shielding will affect the normal bone remodeling and limit the degree of bone restructuring. This could be a factor that lead to aseptic loosening of implants, and implant failure in the long term, especially in acetabular cups. Also, calcium phosphate coatings made from hydroxyapatite powder have a low fracture toughness ( $K_{Ic} = 0.6-1.0 \text{ MPa}\cdot\text{m}^{1/2}$ ). [2]

To modify the mechanical properties of an engineering material, a composite incorporating the advantages of its different components has been employed. As generally known, polymers are usually very ductile, but they are not strong compared to bone (tensile strength is 30 **MPa** for high density polyethylene (HDPE) and 50-150 **MPa** for cortical bone) and they have a modulus (1 **GPa** for HDPE) lower than that of bone. The idea of a **HA/polymer** composite system would, thus, seem promising to provide an optimal combination of the biological and mechanical properties of these two materials.

Bonfield et al. [3] developed a HA reinforced HDPE composite (**HAPEX™**) in the early 1980's by twin screw extrusion, which demonstrated an optimum combination of modulus, toughness and bioactivity when 40% HA by volume was adopted. [4,5] The present study aims to produce a HA and polymer composite coating using flame spray technique. Due to the lack of functional groups, such as -OH, C=O and COOH in its structure, the generally used polyethylene [(-CH<sub>2</sub>-CH<sub>2</sub>-)<sub>n</sub>] was not chosen for this flame spraying technique due to its poor adherence to metal substrates. Instead, a methacrylic acid (**H<sub>2</sub>C=C(CH<sub>3</sub>)OOH**) (MA) modified polyethylene (EMAA) was used, which includes a reactive COOH pendent group that can increase the adhesion of the polymer to metals. [6]

## Experimental

### Feedstock and Processing

The **fully** crystalline pure spray-dried HA powders were added to the ethylene methacrylic acid copolymer (EMAA) powders at volume ratios of **30:70**, **50:50** and **65:35**, respectively. The mixtures were then blended in a cylindrical rotating bowl of dimension **6×6×16 mm** at 100 rpm for 24 hours. The HA was provided by Monash University, Australia. The EMAA

powders were obtained from Plastic Flamecoat Systems (PFS, Big Spring, TX) as PF111, which is a copolymer of ethylene modified by 1-10% methacrylic acid. Both composite coatings and pure EMAA coatings were sprayed using a PFS 124 plastic flame spray system. A propane supply (with a pressure at 12 psi) and a compressed air supply (with a pressure at 80 psi) were used to produce the combustion flame, **while the** compressed air supply was also used to fluidize the powders and transport the powders from the fluidized bed to the **gun**. Mild steel substrates were grit-blasted using  $\text{Al}_2\text{O}_3$  grit and cleaned with acetone before spraying. Peel-off coatings were produced by **spraying the** powders onto a Teflon sprayed substrate.

The substrate was pre-heated to around  $95^\circ\text{C}$  before spraying to ensure initial coating coalescence. An **infrared** pyrometer was used to check the temperature of the substrate and the coating before and during spraying. A spray distance of around 30 cm was decided in order to make the tip of the flame just touch the substrate, and the coating temperature was maintained between  $160^\circ\text{C}$  to  $220^\circ\text{C}$  during spraying. This ensured that the coating will not be overheated and adequate deposition efficiency can be achieved. A systematic study on the effects of spraying parameters on the melting and coalescence of the EMAA can be found in Brogan and **Berndt's** work. [7]

#### Characterization and Testing

The morphology of feedstock powders and the surface morphology, polished cross-section and fracture surface of the composite coatings were examined with a **Philips** ISI-SX-30 Scanning Electron Microscope (SEM). The samples were coated with a thin layer of carbon before the examination for electric conduction. The volume of HA in the composite coatings was calculated using NIH image analysis software on an area of around  $190\text{ cm}^2$  of the cross section image ( $100\times$  magnification). Three different areas were selected for each sample. The composite coating was sectioned with a diamond blade using water as a lubricant and polished with a **Struers** autopolisher where the load, polishing time, disk rotation

direction, diamond slurry and lubricant addition rates were controlled. The particle size distribution of the feedstock powders was evaluated using a Honeywell Microtrac **SRA** Laser Particle Analyzer.

An important aspect of bioactivity is the solubility of a compound that releases a biologically relevant ion into the physiological system, such as calcium, phosphorus or silicon. The bioactivity of the HA powders and the composite coatings was evaluated with a calcium ion meter in this study. The sample used was 25 mg for HA powders and  $15\times 15\times 1\text{ mm}$  peel-off coatings for the composites. The bottom and the edges of the coatings were sealed using a silicone sealant (neutral curing) and left in air for 48 hours before they were put into the solution. The release of  $\text{Ca}^{2+}$  ions from the sample in 50 ml **0.1M** Tris(hydroxymethyl)-aminomethane (Tris-buffer, buffered with **HCl** to  $\text{pH} = 7.3$ ) solution at  $\sim 37^\circ\text{C}$  was obtained for the first four hours after the sample was placed in the solution and after two days. A homogeneous was maintained during measurement by stirring (radius of stirrer = **15 mm**) at **300 rpm**.

Tensile testing was conducted using an Instron **1321** with a 50 lbs load cell. The samples were made from the peel-off coatings according to ASTM standard **D 822-91**, [8] which is in the shape of strip with a width of around 8 mm and a thickness of **0.5-1 mm**. The gauge length is fixed by the grip at 50 mm and the crosshead speed is set at 5 mm/min. At least five samples were tested for each coating.

## **Results and Discussion**

### Morphology and Microstructure

The morphology of the two feedstock components (Fig. 1) shows that the EMAA particles are larger and irregular, while HA particles are smaller and quite spherical, and each particle is an agglomeration of many small particles. The particle size distribution of the two powders (Fig. 2) shows that the average particle size of the HA is around one-third of that of the EMAA. This reduces the possibility of powder separation

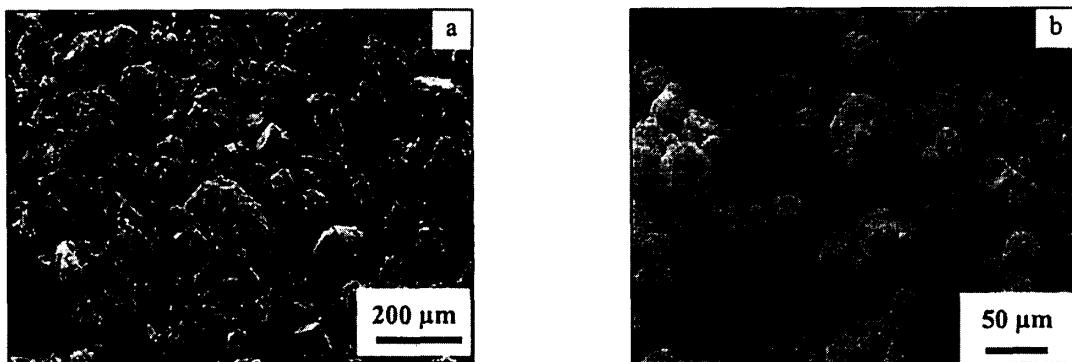


*Figure 1: SEM morphology of EMAA powders (a) and hydroxyapatite powders (b).*

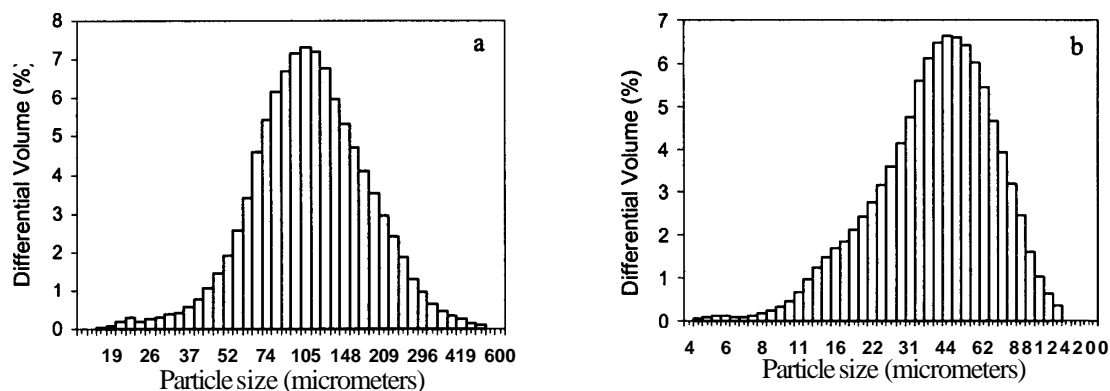


Figure 2: Particle size distribution of EMAA powders (a) and hydroxyapatite powders (b).

when they are fluidized, since the density of the HA ( $\sim 2.9 \text{ g/cm}^3$ ) is much higher than that of the EMAA ( $0.93 \text{ g/cm}^3$ ).

The surface morphologies of the composite coatings are shown in Fig. 3 and the microstructures revealed in Fig. 4. It can be seen that HA particles are distributed in the polymer matrix. Some HA powders were spheroidized into dense particles (usually smaller ones) or crushed into small particles after spraying while others still maintained the original porous characteristics of spray-dried particles. X-ray diffraction of the composite coating shows no phase change for the crystalline

HA after spraying, since the temperature of the propane/compressed air flame (the maximum is  $1300^\circ\text{C}$ ) is not sufficient to melt HA. The surface morphologies of the coatings clearly show both HA particles adhering to the surface and embedded underneath. The microstructure of the coating indicates that some particles were removed during the polishing process; as evidenced by voids in the coating matrix.

The interface between HA particles and the polymer matrix shows good cohesion. However, the actual volume of the HA in the composite coatings is obviously lower than that in the

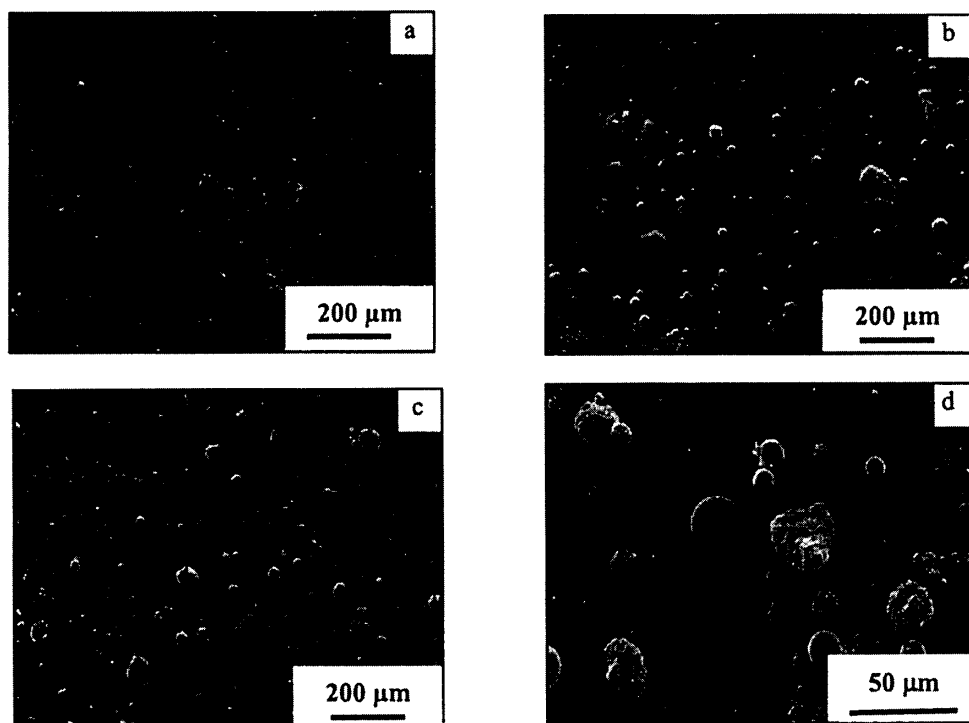
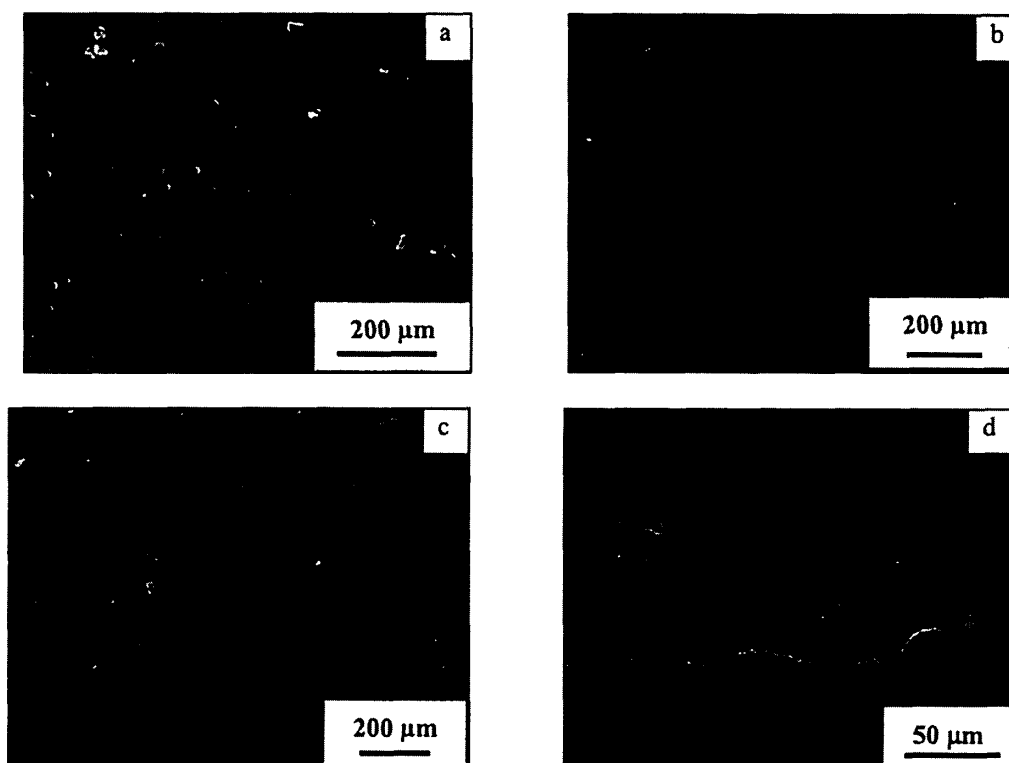


Figure 3: Surface morphologies of composite coatings with HA/EMAA volume ratios (in feedstock) at (a) 30% (b) 50% (c) 65% (d) 65% (high magnification).



**Figure 4: Microstructure of composite coatings with HA/EMAA volume ratio (in feedstock) at (a) 30% (b) 50% (c) 65% (d) 65% (high magnification).**

original feedstock. Calculation by the NIH Image analysis software gave results as  $11 \pm 1.5\%$ ,  $21.5 \pm 2.5\%$  and  $28.5 \pm 3\%$ , which compares with the original formulations of 30%, 50% and 65%. This indicated that much of the HA powder was lost during the spraying process due to the difference in the density and melting properties of these two powders. In addition, the distribution of the HA particles throughout the polymer matrix is not very homogeneous, possibly due to (i) the method of mechanical blending can not evenly mix these two kinds of powders and (ii) the particle size of HA is too large and in a wide range. A more homogeneous composite coating with minimum loss of the HA powders can be formed if a **mechanofused** composite powder (HA as the core and polymer as the shell) [9] or HA with small particle size and distribution [10] is available. Also the flame spray system used in the study, which were originally designed for the EMMA-series powders, needs to be modified to adapt to the composite powders.

#### Bioactivity

The dissolution rates of the HA powders and the composite coatings are shown in Fig. 5. The dissolution rate of the composite coating increased with the volume percentage of the HA and there is some delay before  $\text{Ca}^{2+}$  concentration can be detected. The reason for this delay is not clear. The

dissolution of all coatings increased **after** 2-3 days, and their  $\text{Ca}^{2+}$  concentrations still show the same relationship with the HA volume percentages. However, the  $\text{Ca}^{2+}$  concentrations of

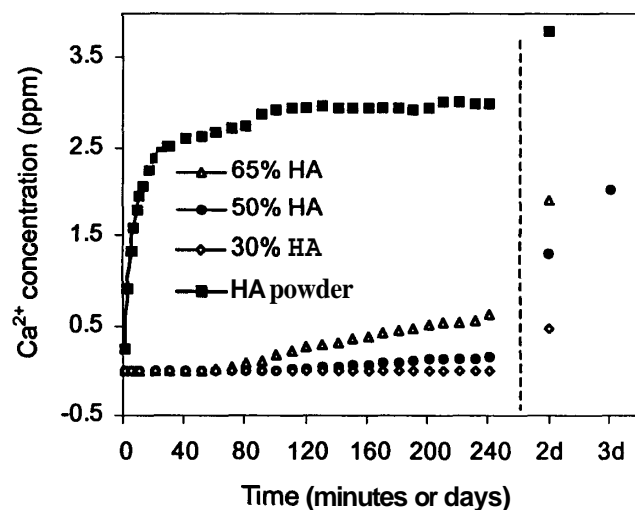


**Figure 5: Dissolution rates of the HA/EMAA composite coatings**  
*Note: The data points on the far right indicate 2 and 3 days.*

all coatings are still lower than that of the feedstock HA powders (3 ppm after 4 hours, 3.8 ppm after 2 days). The surface morphology of the composite coating after the dissolution testing is shown in Fig. 6. It can be seen that the HA particles on the coating surface were all partially dissolved and display an indistinct internal structure of the spray-dried particle while the EMAA matrix seems unaffected by the solution and retains the smooth morphology exhibited before the dissolution testing.

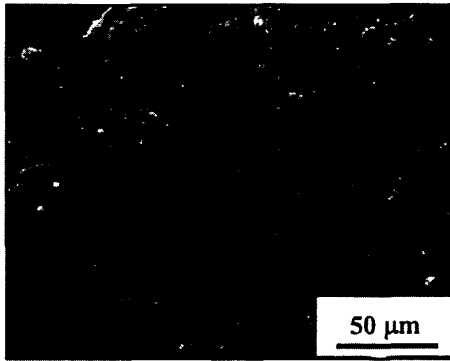


Figure 6: Surface morphology of the HA/EMAA (volume ratio = 50% in feedstock) composite coating after dissolution.

#### Mechanical Property

The stress-strain curves for the pure EMAA coatings and the composite coatings are shown in Fig. 7. It can be seen that the elastic modulus increases with the HA content. Such behavior indicates that the HA particles resist elastic deformation and, thus, the incorporation of the HA particles in the coating increases the Young's modulus, as shown in Fig. 8.

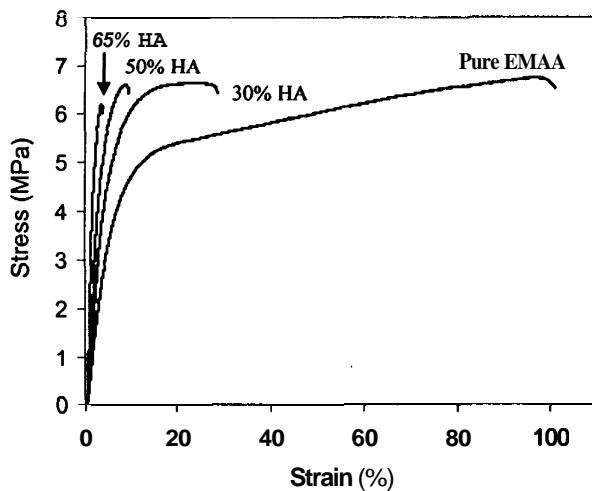


Figure 7: Stress-strain curves of the pure EMAA and HA/EMAA composite coatings.

On the other hand, the elongation of the coatings decreased significantly with the addition of the HA and continues to decrease with an increase of the HA percentage (Fig. 8). The same trend is held for the tensile strength (Fig. 8), although not as significantly as for the elongation. It can be noted, however, that for the composite coatings, all failures occurred at where the sample was gripped. As well, unlike the generally used dog-bone shape, the strip-shaped sample used in this testing did not have a narrower gauge length. The composite coatings were not as ductile as pure EMAA coatings, and the tightening of the grip increased the stress concentration in this region of the sample, which led to the early failure at these locations. Thus, this test protocol only allows comparative measurements of elongation and tensile strength for the composite coatings.

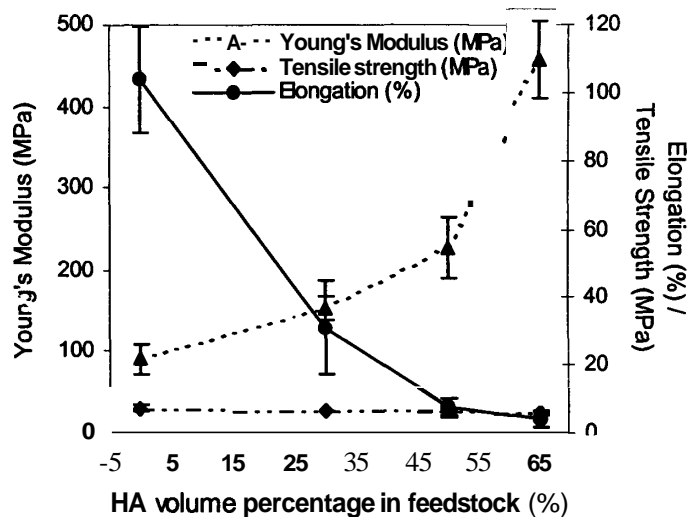


Figure 8: Mechanical properties of the pure EMAA and HA/EMAA composite coatings.

Some testing was also performed following ASTM838-98, [11] where the dog-bone shaped samples were used. Both the elongation and tensile strength show similar trends with the percentage of HA in the composite coating, but were higher than their counterparts in this testing. However, only several samples have been tested according to this standard.

The fracture surface of the HA/EMAA composite coating (Fig. 9) indicates that the HA particles (both spheroidized and agglomerated) were the prime locations for the fracture, as mirrored by the high percentage HA particles in the fracture surface. As well, the cohesion between HA particles and the EMAA matrix was probably inadequate to transfer the stress during the tensile testing and, therefore, many HA particles were debonded from the EMAA matrix.

## References

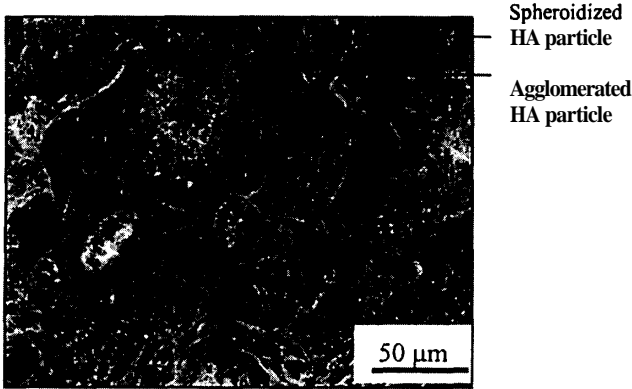


Figure 9: Fracture surface of the HA/EMAA (volume ratio = 50% in feedstock) composite coating.

## Conclusions

1. Hydroxyapatite/EMAA composite coatings can be produced by flame spraying, which shows good adhesion to metallic substrates, increased Young's modulus, good toughness and reasonable bioactivity.
2. The bioactivity and the Young's modulus of the composite coating increased with the percentage of the incorporated HA, while the elongation decreased with the HA percentage.
3. The fracture surface of the composite coating shows that fracture initiated at the HA particles and the poor cohesion between HA particles and the EMAA matrix could not transfer stress during tensile testing.
4. HA powders were preferentially lost during spraying, which led to less homogeneous coatings and a reduced HA/EMAA ratio in the coating than in the feedstock powders.

## Acknowledgments

This work is supported under NSF 431-0586A and DMR 9632570. The authors would also like to thank Dr. Sang-Ha Leigh and Christienne E. Mancini for their assistance.

1. Bonfield W: in "Engineering applications of new composites," ed. S.A. Paipetis, 17-21; 1988, Oxford, Omega Scientific.
2. Ravaglioli A, Krajewski A and de Portu G, "Problems involved in assessing mechanical behavior of bioceramics," in Bioceramics Vol. 1, ed. Oonishi, Aoki and Sawai K, 13-18; 1989, Kyoto, Japan.
3. Bonfield W, Grynias MD, Tully AE, Bowman J and Abram J, "Hydroxyapatite reinforced polyethylene – a mechanically compatible implant material for bone replacement," *Biomaterials*. 2 (1981) 185-86.
4. Bonfield W, "Hydroxyapatite reinforced polyethylene as an analogous material for bone replacement." *Ann NY Acad Sci*. 523 (1988) 173-77.
5. Wang M, Porter D and Bonfield W, "Processing, characterization, and evaluation of hydroxyapatite reinforced polyethylene composites," *British Ceram Trans*. 93(3) (1994) 91-95.
6. Sugama T, Kawase R, Berndt CC and Herman, "An evaluation of methacrylic acid-modified poly(ethylene) coatings applied by flame spray technology," *Progress in Organic coatings*. 25 (1995) 205-16.
7. Brogan JA and Berndt CC, "The coalescence of combustion-sprayed ethylene-methacrylic acid copolymer," *J Mater Sci*. 32 (1997) 2099-106.
8. ASTM standard D822-91. Standard test methods for tensile properties of thin plastic sheet. Annual Book of ASTM standards vol 08.01 (1992) ASTM, Philadelphia, PA. p 313-21.
9. Brogan JA, Gross KA, Chen Z, Berndt CC and Herman H, "Investigation of combustion sprayed hydroxyapatite /polymer composite coatings," pp. 159-64 in Proceedings of the 7<sup>th</sup> National Thermal Spray Conference, June 20-24, 1994, Boston, MA.
10. Wang M, Joseph R and Bonfield W, "Hydroxyapatite-polyethylene composites for bone substitution: effects of ceramic particle size and morphology," *Biomaterials*. 19 (1998) 2357-66.
11. ASTM standard D638-98. Standard test methods for tensile properties of thin plastic sheet. Standard test methods for tensile properties of thin plastic sheet. Annual Book of ASTM standards vol 08.01 (1998) ASTM, Philadelphia, PA. p 45-57.